

28. Run-off transcription procedures were as described (19). The *znu* transcription template was prepared in the same manner as the *zntA* template in (19) and digested with Bsp MI and Bbv I to make a 233-bp fragment. Different size templates were tested for Zur transcription assays and a transcript was always observed for *znuCB* but not *znuA*. Both promoters are active in vivo (16, 17). The *znuCB* promoter may be favored in in vitro transcription because it is stronger than the *znuA* promoter.
29. Y. Hitomi, C. E. Outten, T. V. O'Halloran, in preparation.
30. F. C. Neidhardt, J. L. Ingraham, M. Schaechter, *Physiology of the Bacterial Cell: A Molecular Approach* (Sinauer Associates, Sunderland, MA, 1990).
31. T. Ali Azam, A. Iwata, A. Nishimura, S. Ueda, A. Ishihama, *J. Bacteriol.* **181**, 6361 (1999).
32. J. Granger, N. M. Price, *Limnol. Oceanogr.* **44**, 541 (1999).
33. T. D. Rae, P. J. Schmidt, R. A. Pufahl, V. C. Culotta, T. V. O'Halloran, *Science* **284**, 805 (1999).
34. D. A. Suhy, K. D. Simon, D. I. Linzer, T. V. O'Halloran, *J. Biol. Chem.* **274**, 9183 (1999).
35. M. S. Nasir et al., *J. Biol. Inorg. Chem.* **4**, 775 (1999).
36. D. L. Huffman, T. V. O'Halloran, *J. Biol. Chem.* **275**, 18611 (2000).
37. K. A. Datsenko, B. L. Wanner, *Proc. Natl. Acad. Sci. U.S.A.* **97**, 6640 (2000).
38. F. M. Ausubel et al., Eds., *Current Protocols in Molecular Biology* (Wiley, New York, 1995), vol. 1.
39. F. W. Outten, unpublished data.
40. Supported by NIH training grant T32 GM08382 (C.E.O.) and NIH grants R01 GM38784 and DK52627 (T.V.O.). We thank F. W. Outten for *znuC* primer extension data, S. Shafae for ICP-MS assistance, and Y. Hitomi, H. Godwin, and J. Widom for helpful discussions.

1 March 2001; accepted 24 May 2001
 Published online 7 June 2001;
 10.1126/science.1060331
 Include this information when citing this paper.

Contribution of Aerobic Photoheterotrophic Bacteria to the Carbon Cycle in the Ocean

Zbigniew S. Kolber,^{1*} F. Gerald Plumley,² Andrew S. Lang,³ J. Thomas Beatty,³ Robert E. Blankenship,⁴ Cindy L. VanDover,⁵ Costantino Vetriani,¹ Michal Koblizek,¹ Christopher Rathgeber,⁶ Paul G. Falkowski^{1,7}

The vertical distribution of bacteriochlorophyll *a*, the numbers of infrared fluorescent cells, and the variable fluorescence signal at 880 nanometers wavelength, all indicate that photosynthetically competent anoxygenic phototrophic bacteria are abundant in the upper open ocean and comprise at least 11% of the total microbial community. These organisms are facultative photoheterotrophs, metabolizing organic carbon when available, but are capable of photosynthetic light utilization when organic carbon is scarce. They are globally distributed in the euphotic zone and represent a hitherto unrecognized component of the marine microbial community that appears to be critical to the cycling of both organic and inorganic carbon in the ocean.

Although closely related to purple photosynthetic bacteria, aerobic anoxygenic photoheterotrophs (AAPs) are obligate aerobes, with unusually high concentrations of carotenoids (1–3), low cellular contents of bacteriochlorophyll *a* (BChl*a*) (4), and while containing photosynthetic reaction centers (RC) and light harvesting complex I (LHI), they often lack LHII (3). Photosynthetic energy conversion has been confirmed in several species (5–8), but most known AAPs have been isolated from organic-rich environments (9–11),

where they appear to be heterotrophic. Recently, AAPs were found throughout the surface waters of the oligotrophic ocean (12), however, their abundance, distribution, and potential ecological importance were unknown. Here, we report quantitative measurements of the vertical distribution of AAPs and BChl*a* in the open ocean, determine the photosynthetic competence of these organisms, and evaluate their contribution to the marine carbon cycle.

To characterize the vertical distributions of AAPs and their photosynthetic properties we used an Infrared Fast Repetition Rate (IRFR) fluorescence transient technique (12, 13). Samples obtained from discrete depths were analyzed within 60 min of sampling (14). We assessed the distribution of AAPs using the BChl*a* fluorescence signal at 880 nm (Fig. 1A), and measured bulk BChl*a* by high-performance liquid chromatography (HPLC) (15) (Figs. 1A and 2A). The BChl*a* concentrations reached a maximum of 3 to 5 ng/liter at about 30 m and decreased to levels <0.01 ng/liter below 150 m (Fig. 1A). Chlorophyll *a* (Chl*a*), which in the open ocean is only found in oxygenic phytoplankton, was about 150-fold more abundant. The vertical

distribution of Chl*a*, however, was closely correlated with BChl*a* (Fig. 1B). The HPLC-based estimates of BChl*a* corresponded to the in vivo fluorescence at 880 nm, allowing us to use the IRFR signal (which reflects the radiative losses from LH antennae), to derive the concentration of BChl*a* in situ and vice versa.

To quantify the representation of AAPs, we counted the BChl*a*-containing and total, 4',6'-diamidino-2-phenylindole (DAPI) stained cell numbers by epifluorescence microscopy (16) (Fig. 1C). Model II regression analysis of the relationship between the fluorescence signals, pigment concentrations, and cell counts reveals a significant correlation between the 880-nm fluorescence emission and BChl*a* ($r^2 = 0.68$, $F = 62.6$, Fig. 3A), and the IR fluorescent cell counts ($r^2 = 0.49$, $F = 21.6$, Fig. 3B). From these data, we calculated the average cellular BChl*a* content at 1.2×10^{-19} mol per cell. The morphology of a representative isolate from the surface waters (cylindrical motile cells, approximately 1.2 μm long, 0.7 μm in diameter) allows us to estimate the cell volume at about 0.5 μm^3 , a cell wet weight of 0.5 pg, and a cell dry weight of 0.05 pg, yielding a BChl*a*/dry weight ratio of about 2.4 $\mu\text{mol/g}$. This ratio is similar to that of *Erythrobacter longus* (17), but much higher than that of *Citromicrobium bathyomarimum* (18). Assuming 36 BChl*a* molecules/RC+LHI (19), we estimated about 2000 RCs per cell. The cellular BChl*a* content calculated here is about an order of magnitude lower than that of *Rhodobacter sphaeroides* (20), and the BChl*a*/RC ratio is also about fivefold less than that of typical purple nonsulfur bacteria (19). However, the effective photosynthetic absorption cross section measured at 470 nm (12) (about 62 \AA^2) was comparable to that measured in a laboratory culture of *R. sphaeroides* (about 70 \AA^2). By comparison, the effective absorption cross section in photosystem II reaction centers in phytoplankton averaged 420 \AA^2 , consistent with 200 to 300 Chl*a*/RCII. Although the rate of photon absorption/RC was sevenfold less than in their oxygenic planktonic counterparts, AAPs display a similar light utilization efficiency per unit of chromophore.

Fluorescence excitation spectra, recorded at the emission maximum of 875 nm (21)

¹Environmental Biophysics and Molecular Ecology Program, Institute of Marine and Coastal Sciences, Rutgers University, 71 Dudley Road, New Brunswick, NJ 08901–8521, USA. ²Institute of Marine Science, University of Alaska, Fairbanks, AK 99775, USA. ³Department of Microbiology and Immunology, University of British Columbia, University Boulevard, Vancouver, BC, Canada V6T 1Z3. ⁴Department of Chemistry and Biochemistry, Arizona State University, Tempe, AZ 85287–1604, USA. ⁵Biology Department, College of William & Mary, Williamsburg, VA 23187, USA. ⁶Department of Microbiology, University of Manitoba, 407 Buller Building, Winnipeg, MB, Canada R3T 2N2. ⁷Department of Geology, Rutgers University, 610 Taylor Road, Piscataway, NJ 08854–8066, USA.

*To whom correspondence should be addressed. E-mail: zkolber@imcs.rutgers.edu

REPORTS

(Fig. 2B), indicate that the oceanic AAPs utilize carotenoids as an efficient, auxiliary photosynthetic pigment. These carotenoids harvest light between 460 and 550 nm (Fig. 3B), which penetrates relatively deeply into the water column, whereas infrared light in the 800- to 900-nm range is about 1000-fold attenuated owing to absorption by water (22). The efficiency of excitation transfer from carotenoids to RC (defined as the ratio of quanta transferred to the RC to the quanta absorbed) measured on our isolates of AAPs (Fig. 2B) was relatively low, increasing from approximately 5 to 20% as the organic content in the growth medium decreased. From the IRFRR data acquired in natural AAP populations, we estimated the maximal cellular photosynthetic fluxes at about 1×10^{10} photons, or 2.2×10^{-9} J per cell per day. Assuming a cellular carbon content of about 2.5 fmol (60% of cell dry weight), the maximal cellular photosynthetic energy fluxes could reach 1×10^6 J/mol of carbon under

high irradiance levels, and average 1×10^5 J/mol of carbon in the euphotic zone. Assuming a specific growth rate of one cell per day, and a respiratory efficiency of 5×10^5 J/mol carbon, about 20% of the cellular energy requirement would be satisfied by photosynthetic electron transport.

Oceanic AAPs are capable of light-dependent CO_2 fixation (23) (Fig. 2C). Under saturating light, the rates of light-dependent CO_2 fixation in laboratory-grown isolates are relatively low, averaging at about 0.43 mol carbon/mol RC/s, with a maximum quantum yield of about 1% (mol carbon/mol quanta absorbed). These yields are about an order of magnitude lower than in phytoplankton, and comparable to that reported previously in *Erythrobacter* sp. (24). We estimate the daily

cellular rates of CO_2 fixation at about 0.08 fmol of carbon, or 3% of the cellular carbon content. As the cells were grown in 2 to 20 mM organic medium, maintaining specific growth rates of four per day, CO_2 fixation contributed to about 1% of the total carbon anabolism. In the open ocean, where dissolved organic matter (DOM) is three orders of magnitude less abundant, the relative contribution of the CO_2 fixation may be significantly higher. Nevertheless, the potential contribution of AAPs to the oceanic carbon cycle is determined by their ability to supplement, or substitute respiration with the light-driven generation of ATP and reductants for carbon anabolism, preserving the existing organic carbon. Isolates of oceanic AAPs grown in 20 mM organic medium displayed

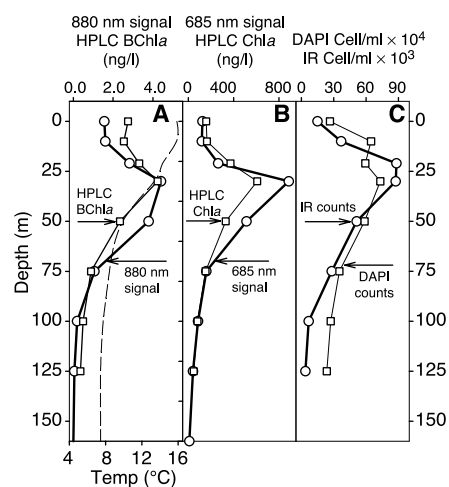
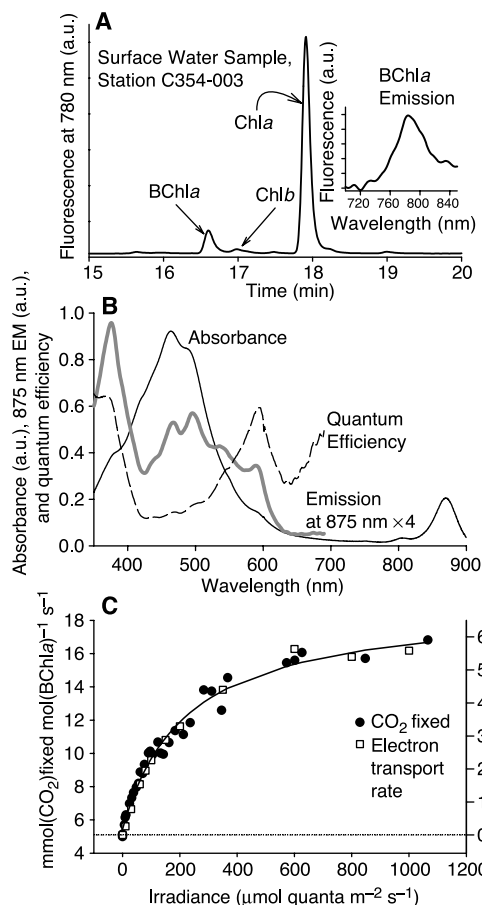
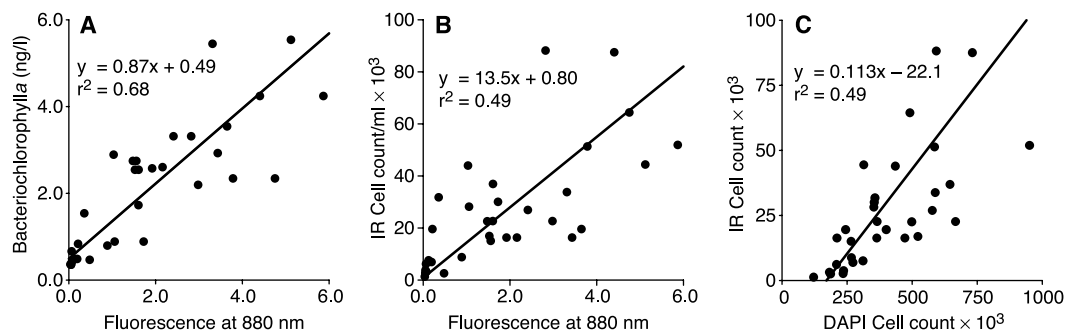


Fig. 1. Vertical distribution of fluorescence, Chla, BChla, and microbial cells on July 2000 at station C354-004. (A) Amplitude of the 880-nm fluorescence signal characteristic of AAPs phototrophic bacteria (○), the corresponding HPLC-based BChla distribution (□), and temperature (broken line). (B) Amplitude of the 685-nm signal characteristic of oxygenic phytoplankton (○) and HPLC-based Chla (□). (C) Infrared cell counts (○) and DAPI stained cell counts (□).

Fig. 3. Relationships between fluorescence, pigment, and cell counts at four stations in the vicinity of the Juan de Fuca Ridge. (A) Model II regression analysis of HPLC-based BChla and fluorescence signal at 880 nm. (B) Model II regression analysis infrared epifluorescence cell count and fluorescence signal at 880 nm. (C) Model II regression analysis of infrared and DAPI-stained cell counts.



REPORTS

about 20 to 40% higher specific growth rate under day-night cycle relative to dark-incubated cultures, resulting in a fivefold higher biomass accumulation within 6 days. Such a mechanism of light-enhanced preservation of the organic carbon will affect the extent of the new production in the upper ocean, given that AAPs are abundant within the microbial community.

Numerically, AAPs constitute approximately $11.3 \pm 1.7\%$ of the total microbial community in the euphotic zone in the Northeastern Pacific Ocean at 48°N, 128°W (Figs. 1C and 3C). The Bchl_a/Chl_a ratio at this location, about 0.8%, increased to as much as 10% in the oligotrophic waters of the Eastern Pacific Ocean at 14°N, 104°W (12). Such a dramatic change in the Bchl_a/Chl_a ratio almost certainly reflects an increase in the relative abundance of AAPs within the microbial community. Thus, the calculated 11.3% of the total cell count at 14°N, 104°W may be greatly exceeded in the oligotrophic ocean, and the globally averaged Bchl_a/Chl_a ratio may be as high as 5 to 10%.

We isolated 10 AAP strains from the Coastal North Atlantic Ocean, Northeastern Pacific Ocean, Equatorial Pacific Ocean, Southern Ocean, and Mediterranean Sea (25). After 8 to 10 days incubation on organic-poor agar plates in the dark, they all formed small pink colonies, which on replating with the same medium frequently segregated into purple and yellow isolates.

When grown in an organic-poor, autotrophic liquid medium, all the isolates displayed IRFRR fluorescence transients characteristic of photosynthetic electron transport, similar to that measured in the natural water samples. When transferred to an organic-rich medium, the purple isolates displayed a 40% decline in the amplitude of the IRFRR fluorescence transient within 24 hours, whereas the yellow isolates lost this signal completely, showing no accumulation of Bchl_a and RC despite maintaining high specific growth rates of about six per day. The growth rate decreased during the next 7 days as nutrients became depleted, the fluorescence transients were restored in both isolates, and Bchl_a accumulation resumed. Such a response to nutrient conditions indicates that oceanic AAPs are capable of controlling the expression of their photosynthetic apparatus; i.e., they are facultative phototrophs, switching to a mostly heterotrophic metabolism under organic-rich conditions, where photosynthesis presumably offers less of an advantage. We observed this behavior within a dense particle layer in the upper portion of the euphotic zone, where we detected a strong fluorescence signal at 880 nm, but with unusually low amplitude of the variable fluorescence.

Phylogenetic analysis of the 16S ribosomal RNA gene (16S rDNA) (26) from a North

Atlantic isolate (NAP1) placed it in the *Erythrobacter-Citromicrobium-Porphyrbacter* cluster within the α -4 subclass of the Proteobacteria (3), which forms a relatively isolated group with respect to other AAPs (27). The 16S rDNA sequence of NAP1 showed high sequence similarity with those of *Erythrobacter longus* and *Erythrobacter litoralis* (98.2 and 97.9%, respectively), suggesting that this isolate belongs to the *Erythrobacter* genus. A preliminary characterization of a purple isolate from the Northeastern Pacific Ocean (NPP1), based on both the restriction fragment length polymorphism (RFLP) and sequence of the 16S rDNA, revealed that this isolate is closely related to NAP1.

Our data indicate that, like cyanobacteria, AAPs are ubiquitous in the euphotic zone of the open ocean. We have observed IRFRR fluorescence transients characteristic of bacterial photosynthesis in every ocean surface water sample analyzed to date. All of these water samples yielded isolates displaying similar fluorescence characteristics. The isolates from the Northeastern Pacific and coastal North Atlantic Oceans, (the most extensively characterized) are morphologically, biophysically and phylogenetically similar. Oceanic AAPs occupy a uniform environment characterized by relatively low concentrations of DOM, and are exposed to high irradiance levels. They are photosynthetically competent in situ and utilize carotenoids as a major LH pigment. All are readily cultivated on organic-poor media. These common features suggest that oceanic AAPs are probably represented by a relatively uniform, widespread class.

We speculate that the phylogenetically related, yet phenotypically diverse aerobic anoxygenic photosynthetic bacteria, discovered in a variety of ecological niches over the last 20 years, may have speciated from a common ancestral oceanic AAP. Possible evolutionary adaptations may have ranged from a permanent loss of photosynthetic activity to the development of a regulatory mechanism that controls the level of expression of the photosynthetic apparatus in response to nutrient concentrations.

The close correlation between AAPs and oxygenic phototrophs in the euphotic zone indicates that they coexist in a tightly linked nutrient cycle. Because AAPs are unable to utilize water as an electron donor, they most likely rely on exudants produced by oxygenic photoautotrophs to supply reductants. AAPs will use the available DOM if present at sufficient concentration, but are also capable of photosynthetic CO₂ fixation under DOM-deficient conditions. Their photosynthetic efficiency and spectral light utilization is similar to that of the oxygenic phototrophs, further explaining their co-occurrence with phy-

toplankton in the water column. These facultative photoheterotrophs coexist with oxygenic photoautotrophs, contributing to a light-controlled component of microbial carbon and redox cycle, the details of which are presently unknown.

References and Notes

1. Y. Nishimura, S. Mukasa, H. Iizuka, K. Shimada, *Arch. Microbiol.* **152**, 1 (1989).
2. T. Noguchi, H. Hayashi, K. Shimada, S. Takaichi, M. Tasumi, *Photosynth. Res.* **31**, 21 (1992).
3. V. V. Yurkov, J. T. Beatty, *Microbiol. Mol. Biol. Rev.* **62**, 695 (1998).
4. K. Shimada, in *Anoxygenic Photosynthetic Bacteria*, R. E. Blankenship, M. T. Madigan, C. E. Bauer, Eds. (Kluwer Academic, Dordrecht, Netherlands, 1995), pp. 105–122.
5. T. Shiba, *J. Gen. Appl. Microbiol.* **30**, 1313 (1984).
6. V. V. Yurkov, H. Van Gemerden, *Arch. Microbiol.* **159**, 84 (1993).
7. D. Garcia, P. Mathis, A. Vermeglio, *Photosynth. Res.* **55**, 331 (1998).
8. C. Schwarze, A. V. Carluccio, G. Venturoli, A. Labahn, *Eur. J. Biochem.* **267**, 422 (2000).
9. T. Shiba, U. Simidu, N. Taga, *Appl. Environ. Microbiol.* **38**, 43 (1979).
10. T. Shiba, Y. Shioi, K. Takamiya, D. C. Sutton, C. R. Wilkinson, *Appl. Environ. Microbiol.* **57**, 295 (1991).
11. V. Yurkov *et al.*, *Int. J. Syst. Bacteriol.* **44**, 427 (1994).
12. Z. S. Kolber, C. L. Van Dover, R. A. Niederman, P. G. Falkowski, *Nature* **407**, 177 (2000).
13. Z. S. Kolber, O. Prasil, P. G. Falkowski, *Biochim. Biophys. Acta* **1367**, 88 (1998).
14. We occupied five stations over a 14-day period in the Northeast Pacific, off the Washington and Oregon coasts in July 2000 onboard the R/V *Atlantis*.
15. Water samples (1 liter) were filtered through GF/F filters. Filters were extracted briefly in 100% acetone, then water was added to yield 1 ml of 80% acetone. Pigments were extracted for 6 to 8 hours at –20°C and debris removed by centrifugation at 14,000g for 10 min. 100 μ l of extract was injected into an Agilent Technologies HPLC Model 1100 equipped with a Microsorb-MV (Rainin Instruments) C18 column (4.6 \times 250 mm). The initial mobile phase was 75% acetone for 3 min and ramped to 100% acetone over 15 min. The fluorescence detector was equipped with a Hamamatsu R928 photomultiplier tube, which proved to be crucial for detection of Bchl_a. Excitation was set at 365 nm, emission at 780 nm, and slits were 20 nm. These wavelengths maximized signals from Bchl_a and minimized those from the more abundant pigments, Chl_a and Chl_b. Acetone extracts from lettuce and *R. sphaeroides* served as standards. An extinction coefficient $\epsilon_{770} = 60$ was used for Bchl_a [J. Oelze, *Methods Microbiol.* **18**, 257 (1985)].
16. Water samples of 10 ml were stained with 0.1 mg/ml 4'6-diamidino-2-phenylindole (DAPI) [K. G. Porter, Y. S. Feig, *Limnol. Oceanogr.* **25**, 943 (1980)], and cells were collected by filtration through 0.2 μ m pore size polycarbonate membranes. DAPI-stained particles in five fields (field size $1.4 \times 10^4 \mu\text{m}^2$) were enumerated using epifluorescence with the following filter set: excitation 330 to 390 nm, emission 440 to 490 nm, beam splitter 400 to 430 nm. Infrared fluorescent cells, diagnostic of the presence of Bchl, were counted from five fields (field size $3.3 \times 10^4 \mu\text{m}^2$) using the following filter set: excitation 350 to 550 nm, emission >850 nm, beam splitter 650 nm, and viewed with an IR-sensitive CCD camera. The five values obtained for each were averaged and multiplied by appropriate factors to yield cell concentrations in the original samples.
17. K. Harashima, J. Haayasaki, T. Ikari, T. Shiba, *Plant Cell Physiol.* **21**, 1283 (1980).
18. V. V. Yurkov, S. Krieger, E. Stackebrandt, J. T. Beatty, *J. Bacteriol.* **181**, 4517 (1999).
19. H. Zuber, R. J. Cogdell, in (4), pp. 315–348.
20. J. Takemoto, M. Kao, *J. Bacteriol.* **129**, 1102 (1977).
21. Cells were grown in liquid autotrophic medium enriched with 0.2 g of yeast extract and 0.1 g of peptone per liter, to a concentration of about 10^9

cells per milliliter. Excitation spectra were measured in 70% glycerol using an Aminco Series 2 spectrofluorometer equipped with a R928 photomultiplier. The excitation monochromator was operated with a 4-nm slit, and the emission monochromator was operated at 875 nm with a 16-nm slit, and protected by a Shott RG830 glass filter.

22. A. Morel, D. Antoine, *J. Phys. Oceanogr.* **24**, 1652 (1994).

23. CO₂ fixation measurements were performed with NAP1 isolate diluted to 30 nM BChla concentration, at 25°C. Aliquots of 2 ml were labeled by addition of 2 μCi of NaH¹⁴C₃ (New England Nuclear) and exposed to 36 light intensities provided by a quartz halogen lamp attenuated by a set of neutral density filters. After incubation, the samples were killed by addition of 30 μl of 36% HCl and evaporated to dryness. The samples were resuspended in 2 ml of 30 mM Tris buffer (pH 7.7) and 15 ml of scintillation cocktail (Ready Safe, Beckman). The incorporated radioactivity was determined using Beckman LS6K-IC scintillation counter, and corrected for blank and dark counts.

24. T. Shiba, *J. Gen. Appl. Microbiol.* **30**, 1313 (1984).

25. Water samples of 50 μl collected from the surface, and from depths corresponding to the maximum amplitude of 880 nm IRFRR signal were spread on f/2 agar plates, incubated in darkness for 6 days, and then exposed to ambient light with a 14/10 hours day/night cycle. Small, about 0.5-mm-diameter col-

onies of gray, green, yellow, and pink color appeared within 8 to 10 days of incubation. Among these, only the pink colonies displayed the fluorescence transients at 880 nm. Following two to three plate transfers, the isolates were transferred to a liquid f/2 medium enriched with 0.2 g/liter yeast extract and 0.1 g/liter peptone. The BChla accumulation was followed by using the IRFRR signal. Grown on a shaker under ambient, natural illumination, the pink isolates displayed a maximum specific growth rate, estimated from BChla accumulation, of about four per day. BChla accumulation was observed only during the dark period, and was retarded during the day.

26. NAP1 genomic DNA was isolated from 5.0 ml of culture. Cells were subjected to both physical (repeated freeze-thawing) and enzymatic lysis, and the DNA was extracted with phenol chloroform and precipitated with 300 mM sodium acetate and 70% ethanol. Polymerase chain reaction (PCR) was performed to amplify the 16S rDNA using primers S-D-Bact-0008-a-S-20 (5'-AGAGTTTGATCCTGCTCAG-3') [R. E. Hicks, R. I. Amann, D. A. Stahl, *Appl. Environ. Microbiol.* **58**, 158 (1992)] and S*-Univ-1517-a-A-21 (5'-ACGGCTACCTTGTTACGACTT-3') [W. G. Weisburg, S. M. Barns, D. A. Pelletier, D. J. Lane, *J. Bacteriol.* **173**, 697 (1991)]. PCR products were gel-purified, cloned in the PCR II plasmid vector (Invitrogen, Carlsbad, CA) and their sequences were determined on an ABI 310

Automated Sequencer (Applied Biosystems, Foster City, CA). Sequences were aligned manually to 16S rRNA sequence data from the RDP [N. Larsen *et al.*, *Nucleic Acids Res.* **21**, 3021 (1993)] and recent GenBank releases using the Genetic Data Environment (GDE) multiple sequence editor. A total of 1366 aligned unambiguous nucleotides were used in the analysis. Maximum-likelihood trees were constructed using fastDNAm1 [J. Felsenstein, *J. Mol. Evol.* **17**, 368 (1981)], which uses the generalized two-parameters model of evolution [H. Kishino, M. Hasegawa, *J. Mol. Evol.* **29**, 170 (1989)], and using jumbled orders for the addition of taxa to avoid potential bias introduced by the order of sequence addition. Transition/transversion ratios were optimized and bootstrap analysis was used to provide confidence estimates for phylogenetic tree topologies [J. Felsenstein, *Evolution* **19**, 783 (1985)].

27. Supplemental figure is available at *Science Online* at www.sciencemag.org/cgi/content/full/292/5526/2492/DC1

28. This research was sponsored by NASA, NSF, the Office of Naval Research, and NSERC (Canada). We thank the crew of the R/V Atlantis for their service to our scientific research effort at sea.

8 February 2001; accepted 3 May 2001

Nitrogen Fixation by Symbiotic and Free-Living Spirochetes

T. G. Lilburn,^{1,2} K. S. Kim,³ N. E. Ostrom,⁴ K. R. Byzek,³ J. R. Leadbetter,⁵ J. A. Breznak^{3,2*}

Spirochetes from termite hindguts and freshwater sediments possessed homologs of a nitrogenase gene (*nifH*) and exhibited nitrogenase activity, a previously unrecognized metabolic capability in spirochetes. Fixation of 15-dinitrogen was demonstrated with termite gut *Treponema* ZAS-9 and free-living *Spirochaeta aurantia*. Homologs of *nifH* were also present in human oral and bovine ruminal treponemes. Results implicate spirochetes in the nitrogen nutrition of termites, whose food is typically low in nitrogen, and in global nitrogen cycling. These results also proffer spirochetes as a likely origin of certain *nifH*s observed in termite guts and other environments that were not previously attributable to known microbes.

Termites are important terrestrial decomposers of Earth's major form of biomass: lignocellulosic plant material and residues derived from it, e.g., humus (1). However, the carbon-rich but typically nitrogen-poor character of the termite diet has led many species into symbiotic interactions with gut microbes to augment their nitrogen economy. These interactions include the recycling of excretory (uric acid) nitrogen and the acquisition of new nitrogen through N₂ fixation (2). In wood-feeding termites, whose food may con-

tain as little as 0.05% nitrogen (dry weight basis), N₂ fixation can supply up to 60% of the nitrogen in termite biomass (3). Unfortunately, our understanding of N₂-fixing microbes in termites is meager: only a few strains have been isolated (*Citrobacter freundii*, *Pantoea agglomerans*, and *Desulfovibrio* spp.), and their contribution to N₂ fixation in situ is questionable (2). Indeed, recent surveys of the nitrogenase iron-protein encoding gene (*nifH*) in termite guts implied that the diversity of N₂-fixing microbes was far greater than that inferred by pure culture isolation (4–6), and most of the deduced amino acid sequences of NifH differed from those of known microbial taxa (7).

A long-recognized, major, and morphologically distinct component of the termite gut microbiota are spirochetes, whose cloned 16S rDNA gene sequences group them within the genus *Treponema* (8). Recently, the first pure

cultures of these forms were obtained (9). Isolated strains ZAS-1, ZAS-2, and ZAS-9 were also phylogenetically affiliated with the treponemes (Fig. 1), and all three strains produced acetate as a major fermentation product (10). ZAS-1 and ZAS-2 could make acetate from H₂ + CO₂ (9), a mode of energy-yielding metabolism previously unknown in the phylum *Spirochaetes* (11). Hence, they are important to the nutrition of termites, which use microbially produced acetate as a major carbon and energy source (2). Having these spirochetes in culture prompted us to examine whether they might also fix N₂ and thereby contribute to termite nitrogen economy as well. To do this, we examined their genomic DNA for the presence of *nifH* (12) and their ability to fix N₂ (13).

Two *nifH* homologs were found in each termite gut treponeme. *nifH* homologs were also found in the bovine ruminal treponeme, *Treponema bryantii*; the human oral treponemes, *Treponema denticola* and *Treponema pectinovorum*; and the free-living spirochetes, *Spirochaeta aurantia*, *Spirochaeta zuelzeriae*, and *Spirochaeta stenostrepta*. The deduced amino acid sequence of each NifH had motifs typically present in the nitrogenase iron-protein, including conserved cysteines at positions (*Klebsiella pneumoniae* numbering) 86, 98, and 133 [and 39, for *nifH* clones obtained with the IGK forward primer for polymerase chain reaction (PCR)] and an arginine at position 101, which is a site for reversible inactivation by adenosine diphosphate-ribosylation in some bacteria (14). However, the NifHs were phylogenetically diverse and not congruent with spirochete phylogeny based on 16S rRNA sequences, which groups all spirochetes in a single phylum. This lack of congruence extended to multiple NifH homologs in the same spirochete (Fig. 2). One

¹Ribosomal Database Project, ²Center for Microbial Ecology, ³Department of Microbiology and Molecular Genetics, ⁴Department of Geological Sciences, Michigan State University, East Lansing, MI 48824–1101, USA. ⁵Environmental Science and Engineering, California Institute of Technology, Pasadena, CA 91125–7800, USA.

*To whom correspondence should be addressed: E-mail: breznak@msu.edu